Visualization of Underexpanded Jet Structure from Square Nozzle

Seiji TSUTSUMI, Kazuo YAMAGUCHI and Susumu TERAMOTO

The University of Tokyo, Dept. of Aeronautics and Astronautics
7-3-1 Hongo Bunkyo-ku, Tokyo, 113-8656, Japan
E-mail: seiji@thermo.t.u-tokyo.ac.jp

Keywords: Propulsion, Underexpanded Jet, Linear Aerospike Engine

Abstract

Numerical and experimental investigation were carried out to clarify the flow structure of underexpanded jet from a square nozzle. The square nozzle represents one of the clustered combustors of a linear aerospike engine. From the numerical results, the three-dimensional shock wave of the underexpanded square jet was found to be composed of two shocks. One is the intercepting shock which corresponds to the shock observed in two-dimensional planar jet. The other is the recompression shock divided into two types. The expansion fans coming from the nozzle edges interact with each other at the corners of the nozzle exit, and overexpanded regions are generated. Therefore one of the two recompression shocks is formed at the corners of the nozzle exit behind the overexpanded regions. As the jet goes downstream, the overexpanded regions grow larger to coalesce at the symmetry planes. Then, the other type of the recompression shock is generated. The three-dimensional shock structure formed by the intercepting shock and the recompression shocks dominates the expansion of the jet boundary. The shock detection algorithm using CFD results was developed to reveal the relation between the shock waves and the jet boundary, and it was found that the cross-sectional jet shape becomes cross-shape. The key features observed in the numerical investigation were verified by the experimental results. The shock structure at the diagonal plane was in good agreement with the experimental schlieren images. Moreover, the cross-sections visualized by the Mie scattering method confirmed that the cross-section of the jet becomes cross-shape.

Introduction

A linear aerospike engine (Fig.1) is regarded as one of the prominent propulsion systems for SSTO (Single Stage To Orbit). This engine has clustered combustors placed at the inlet of the linear aerospike nozzle, called thrust cell. The throat of the thrust cell must be circular to avoid excessive heat load. On the other hand, the exit of the thrust cell needs to be rectangular, otherwise the gaps between the neighboring thrust cells produce large drags and also cause disturbances over the exhaust flow field. Therefore, cross-section of the

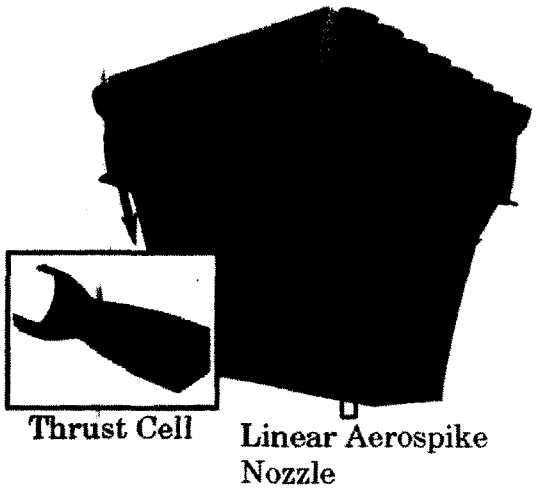

Fig. 1: Linear Aerospike Engine

diverging contour transforms from circular to rectangular as shown in Fig.1. To reveal the interacted flow field on the linear aerospike nozzle, there is a need to clarify the underexpanded jet structure issuing from the rectangular nozzle.

The rectangular jets have been studied extensively and are applied for a passive mixing technique, noise suppression device and thrust vector control. Gutmark et al. summarized the past studies.[1] They revealed the flow characteristics of rectangular subsonic jets. The secondary flow occurs around the corner of the rectangular exit plane and jet boundary in the minor axis plane spreads faster compared to that in the major axis plane. This phenomenon is called axis switching. On the other hand, supersonic jets are dominated by expansion fans and shock waves, and the secondary flow is not so effective. Teshima et al. studied extensively underexpanded jets from rectangular sonic orifices.[2,3] It was observed that the cross-sectional jet shape shows axis switching. Then, once the lateral shocks originating from both ends of the orifice intersects on the flow axis, the jet spreads only in the minor axis plane. However, they didn't clearly explain the reasons causing the observed jet structure from rectangular sonic orifices. Considering the application of the thrust cell to a linear aerospike engine, it is important to clarify the three-dimensional flow structure of underexpanded jets from rectangular nozzles.

The present study aims to understand the structure of underexpanded jets from a square nozzle. Numerical and experimental investigations were carried out. Shock detection algorithm was applied to the Computational Fluid Dynamics (CFD) results to clarify the three-dimensional shock structure. For the experimental investigation, Schieren optical method and Mie scattering method were employed to visualize the jet structure.

Test Nozzle Geometry and Conditions

The square nozzle studied in this study has a circular throat and a square exit. The diameter of the throat:D_t is 6[mm], and the area ratio is set at 2.0 that gives exit Mach number of 2.2 under the assumption of quasi-one-dimensional flow for gaseous nitrogen ($\kappa = 1.4$). The design method and discussions on the exhaust flow field are given in the reference.[4]

Table. 1: Numerical and Experimental Conditions

	NPR	NPRe
Numerical	26.7	2.5
Experimental	27.4	2.56

Table.1 shows experimental and numerical conditions. NPR denotes nozzle pressure ratio ($=P_o/P_a$), and NPRe is defined as the nozzle static pressure ratio at the exit plane ($=P_e/P_a$), where P_o:inlet total pressure, P_e:static pressure at the nozzle exit and P_a:ambient pressure.

Numerical Approach

Numerical Method

The governing equations employed here are the Reynolds-averaged three-dimensional Navier-Stokes equations. Physical properties are normalized by density, sound speed and viscous coefficient at the nozzle inlet stagnation condition. Moreover, length is normalized by the diameter of the throat.

Numerical fluxes for the convective terms are evaluated by the Simple High-resolution Upwind Scheme (SHUS),[5] and it is extended to higher-order by the MUSCL interpolation based on the primitive variables. Since steady-state solutions are only considered, the Lower-Upper Alternating Direction Implicit (LU-ADI) algorithm[6] is employed for time integration.

Under symmetry assumption, a quarter of the flow field is only calculated to analyze the steady-state jet structure of the first shock cell. The computational domain used in the simulation is shown in Fig.2. Near the edge of the nozzle exit plane, a fine domain is located to resolve the rapid expansion of the jet. Large difference of grid spacing between the fine and the coarse global domains causes the mismatch of physical properties at the boundary, therefore, a middle spacing domain is placed between the two. Total number of the grid is about 2 million. The Fortified Solution Algorithm is employed to transfer the computed physical data between the overset or slightly overlapped domains.[7]

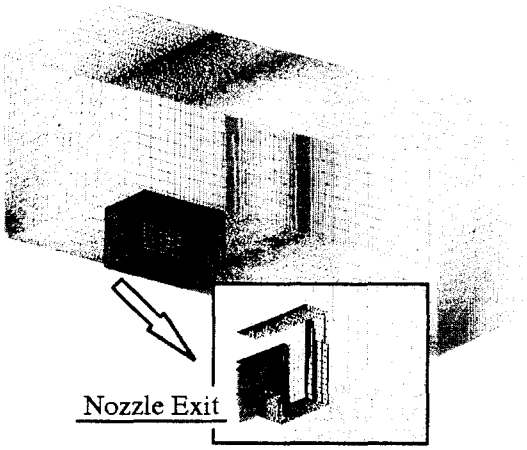

Fig. 2: Computational Domain

The simulations is executed on the HITACHI SR8000/MPP at the University of Tokyo, and the computational code is parallelized by hybrid MPI/OpenMP implementation.

Visualization of Shock Surface

At supersonic jets, generation of expansion fans and shock waves determines the jet boundary. Thus, in this study, visualization of three-dimensional shock structure is required to analyze the flow field.

There are two main types of the shock detection algorithms using CFD results. One is based on the Mach number normal to the shock surface (normal Mach number).[8,9] A shock is considered to be located where the normal Mach number exceeds one. The other method employs the gradients of flow properties in the direction of local velocity vector(directional derivative). A shock surface is assumed to be located where the second directional derivative is zero while the first directional derivative is non-zero.[10]

A difficulty in the shock detection algorithms are how to evaluate the normal Mach number or the directional derivatives from numerical results containing noises caused by the dispersion or dissipation and by the lack of resolution of a shock wave. The key issues are the filtering techniques and the selection of threshold values. Therefore, numerical experiments must be carried out to find the best fitted shock detection algorithms including filters and thresholds. In this study, the former method using normal Mach number:M_n is applied.

$$M_n = \vec{M}\frac{\nabla f}{|\nabla f|} = \frac{1}{a}\frac{\mathbf{U}\cdot\nabla f}{|\nabla f|} \qquad (1)$$

f denotes discontinuous physical properties at shock waves. Shock wave exists where $M_n \geq 1$.

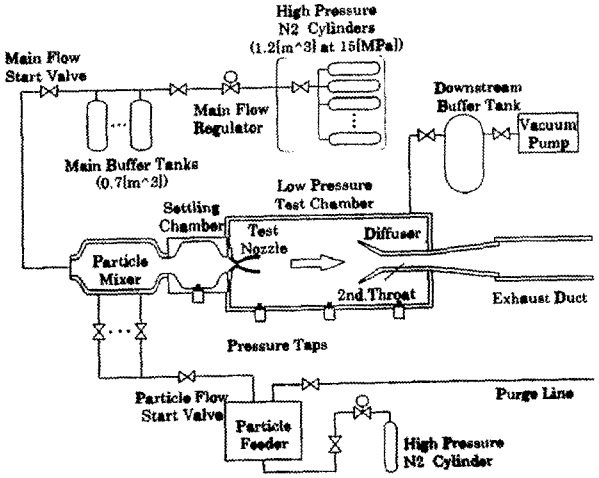

Fig. 3: Simplified Diagram of Experimental Setup

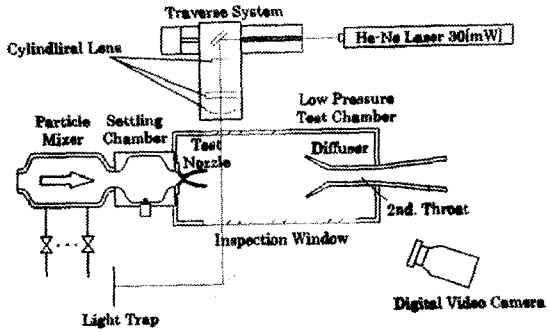

Fig. 4: Optical Arrangement of Mie Scattering Method

Absolute value of local velocity vector is selected as f, i.e., $f = |\mathbf{U}|$. In order to eliminate the physically irrelevant normal vectors caused by the numerical error of $|\nabla f|$ at the uniform flow regions, a filtering technique introduced by Cebral et. al[9] is employed.

$$r = \left| \frac{\nabla |\mathbf{U}|}{g_n} \right|, \quad g_n = \frac{1}{h} \left(c_1 \left| \mathbf{U} \cdot \frac{\nabla |\mathbf{U}|}{|\nabla |\mathbf{U}||} \right| + c_2 |\mathbf{U}| \right) \tag{2}$$

where h is the local characteristic mesh size and $c_1 = O\left(10^{-2}\right), c_2 = O\left(10^{-4}\right)$.

Most of the examples mentioned in the past studies[8,9] employed adapted unstructured grids. The accuracy and smoothness of the captured shock surface is strongly related to the resolution of the grid. However, the present study applies structured grids. Thus the resolution of the oblique shock waves is so poor and the numerical results are interpolated into the finer domain using piecewise linear interpolation based on the values of the nearest eight points.

Experimental Approach

Experimental Setup

A cold-gas blowdown test stand as illustrated in Fig.3 was built for the experiment. 15[MPa], 1.2[m^3] gaseous nitrogen was supplied to the settling chamber through pressure regulator and 0.7[m^3] buffer tank. Inlet total pressure was regulated to less than 2.0[MPa].

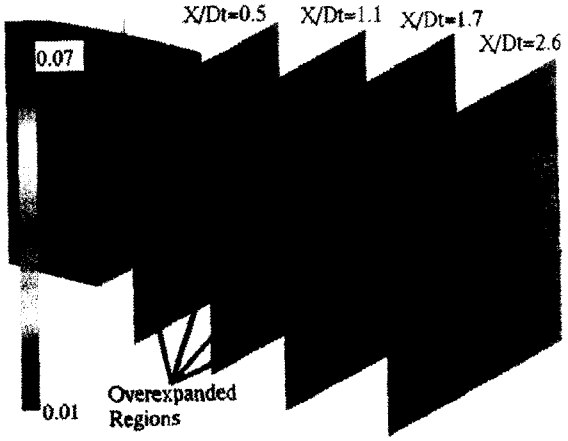

Fig. 5: Cross-Sectional Static Pressure Distribution

The test nozzle mounted on the settling chamber was placed in the low pressure chamber which was depressurized by the exhaust flow ejector system. A exhaust flow ejector system is originally employed in altitude simulation test facilities for upper-stage rocket engines.[11] In this study, however, the supersonic diffuser was located at the downstream enough to keep the exhaust flow to be free jet in the low pressure chamber. Once the exhaust jet reattaches to the inlet of the supersonic diffuser, the diffuser works the same as that of altitude simulation test facilities.

Visualization Techniques

The structure of shock waves was visualized by the schlieren optical method. The images were recorded by the high-speed CCD camera with the shutter-speed of 5[μs] and also by the still camera. Moreover, Mie scattering method using laser light sheet was employed to visualize cross-sectional jet shape. The optical arrangement of the imaging system and the test sections are illustrated in Fig.4. The ash of 2.0[μm] diameter standardized by the Japan Industrial Standard Z8901 was chosen for a scattering particle. The illumination source was a He-Ne laser (30[mW], λ=632.8[nm]), and the scattered images were taken by the Digital Video Camera with the frame-rate of 1/30 second.

Results and Discussion

When a jet is exhausted from a nozzle at underexpanded conditions, expansion fan is generated from the nozzle lip to match the static pressure of the jet to the ambient pressure at the jet boundary. For the square nozzle, expansion fans emanating from the vertical and horizontal nozzle edges interact with each other. Thus the overexpanded regions are produced around four corners of the nozzle exit. Figure.5 shows the numerical result of the static pressure distribution at each cross-sections. From Fig.5, the static pressure

at these regions is found to be lower than the ambient pressure. Thus, recompression shock waves are formed behind these overexpanded regions to recover the static pressure. Figure.6 indicates the density contours of the numerical result at the symmetry (a) and the diagonal (b) planes. Figure.6 (b) shows the recompression shock extending from the nozzle edge.

As the jet goes downstream, the overexpanded regions grow larger and then intersect with each other at X/D_t=1.7 as shown in Fig.5, where X denotes the distance from the nozzle exit plane and D_t represents the throat diameter. Then, another recompression shock waves emerges at the symmetry plane. The oblique shock wave appeared at the symmetry plane (Fig.6 (a)) corresponds to the recompression shock wave.

For underexpanded jets from two-dimensional planar nozzles, the expansion fan extends to the jet boundary and then reflects as the compression waves. Then, these compression waves coalesce to form the intercepting shock wave. The underexpanded jet from the square nozzle also has the intercepting shock as indicated in Fig.6 for the same reason as two-dimensional planar jets.

Figure.7 is the experimental schlieren picture at the diagonal plane for NPRe=2.56 taken by the still camera with the shutter-speed of 0.5[ms]. Three-dimensional shock structures can't be visualized by the schlieren optical method in principle, because the density gradient is integrated along the light path. Nevertheless, the recompression shocks extending from the nozzle edge and their intersection are in good agreement with the numerical result.

As a result, the shock structure of the underexpanded square jet is found to be composed of the recompression shock wave and the intercepting shock wave. Figure.8 shows shock surface painted with the density gradient magnitude as an indication of shock strength. At first, recompression shocks appear around the four corners of the nozzle exit plane. Then, these recompression shocks disappear due to the interference with the expansion fans from the nozzle edges or due to the grid resolution. At the downstream, recompression shocks reappears at the symmetry planes. Moreover, following the recompression shocks, there are the intercepting shocks corresponding to the raised portions indicated in Fig.8. Then, the intercepting shocks are united with the recompression shocks which intersect regularly.

The three-dimensional shock structure indicated in Fig.8 dominates the expansion of the jet boundary. Figure.9 shows cross-sectional density contours with the shock surface to clarify the relationship between the shock and the jet boundary. Ejected from the nozzle, the jet expands outward through the expansion fans. Thus, the jet boundary around the symmetry planes

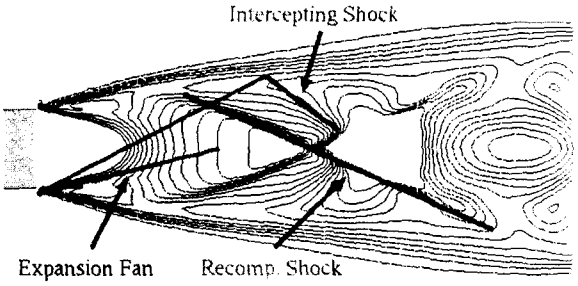

(a) Symmetry Plane

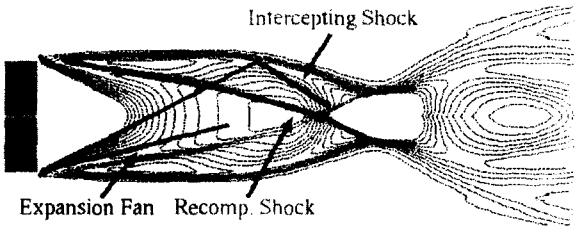

(b) Diagonal Plane

Fig. 6: Schematics of Flow Structure with Density Contour at Symmetry and Diagonal Planes

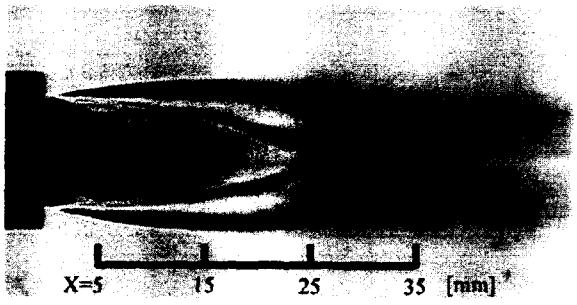

Fig. 7: Experimental Schlieren Picture at Diagonal Plane; Shutter-Speed=0.5[ms]

expands two-dimensionally according to the Prandtl-Meyer's theory, while the jet boundary at the corner regions turns inward through the recompression shock waves. The jet boundary at the symmetry planes still expands two-dimensionally at X/D_t=2.5 in spite of the recompression shocks. At X/D_t=4.2, the jet boundary turns inward furthermore due to the intercepting shocks. Consequently, the cross-sectional jet shape becomes cross-shape as shown in (Fig.9)

From the experiment, the numerical results of the cross-sectional jet shapes are confirmed. Figure.10 is Mie scattering images of the cross-sections. Axial positions of each cross-sections are illustrated in Fig.7. At the axial position of X=5[mm], the jet shape is almost the same as the nozzle exit. Then at X=15[mm], the jet shape starts to be deformed, and at the downstream X=25 and 35[mm], the jet shape grows to become distinct cross-shape.

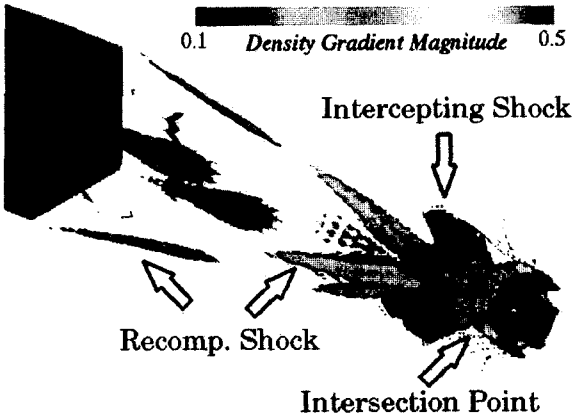

Fig. 8: Shock Surface painted with Density Gradient Magnitude

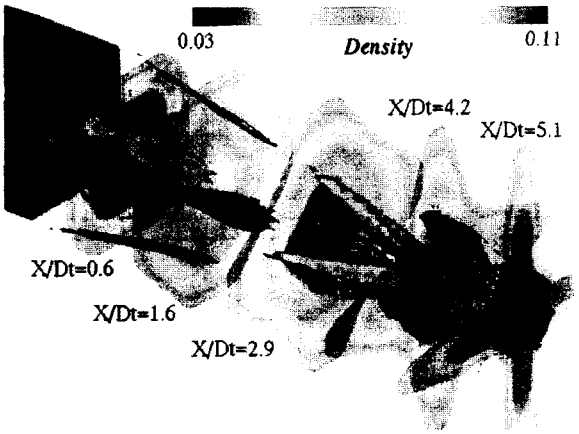

Fig. 9: Shock Surface with Cross-Sectional Density Contour thresholded by Pitot Pressure

Conclusions

The underexpanded jet from the square nozzle representing one of the clustered combustors of the linear aerospike engine was studied numerically and experimentally. From the numerical investigation, it is revealed that the three-dimensional shock wave is composed of the recompression shock waves and the intercepting shock waves. The intercepting shock of the square jet is formed for the same reason as that of two-dimensional planar jets. On the other hand, the recompression shock is generated behind the overexpanded regions at the corners caused by the interaction of expansion fans from the nozzle edges. Moreover, the overexpanded regions grow up to intersect with each other at the symmetry plane, then another recompression shock is formed.

The three-dimensional structure made up of the two shocks is visualized by the shock detection algorithm. Furthermore, the relation between the shock surface and the cross-sectional jet shape is made clear, which explains the reason for the cross-sections of the jet to be cross-shape.

The characteristic features of the square jet is also confirmed by the experimental investigation. The experimental schlieren picture verifies the numerical result of the recompression shock extending from the nozzle edge at the diagonal plane and its intersection point. Furthermore, cross-sectional jet shape visualized by the Mie scattering method demonstrates a tendency to become cross-shape.

Acknowledgement

The authors would like to express the profound appreciation to Hideyuki Oguni, Mioko Sugimoto and Yosuke Kondo (undergraduate students, the University of Tokyo, Dept. of Aeronautics and Astronautics) for their energetic research activities. The experiment in this study was carried out as their graduation thesis. In addition, one of the authors (S.Tsutsumi) was supported through the 21th Century COE Program, "Mechanical System Innovation", by the Ministry of Education, Culture, Sports, Science and Technology.

References

[1] Gutmark, E. J. and Grinstein, F. F., "Flow Control with Noncircular Jets," *Annual Review of Fluid Mechanics*, Vol. 31, 1999, pp. 239–272.

[2] Teshima, K. and Nakatsuji, H., "Structure of Freejets from Slit Orifices," *Rarefied Gas Dynamics*, Vol. 2, edited by V.Boffi and C.Cercignani (Teubner, Stuttgart, 1986), pp. 595–604.

[3] Teshima, K., "Two-dimensional Focusing of a Supersonic Free Jet by a Rectangular Orifices," *Physics of Fluids*, Vol. 30, 1987, pp. 1899–1901.

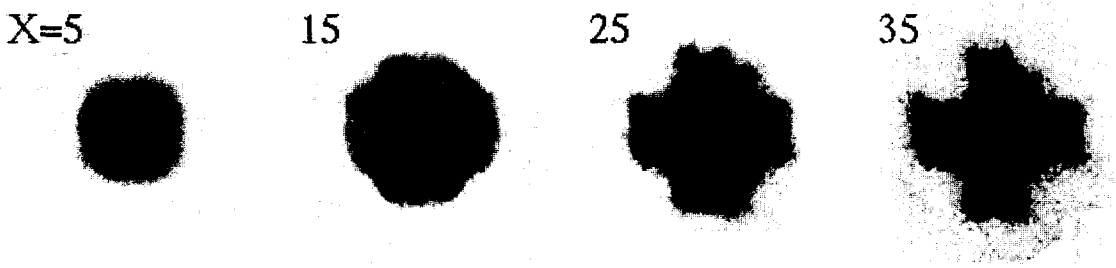

Fig. 10: Mie Scattering Image of Cross-Sections; Axial Positions are specified in Fig.7

[4] Tsutsumi, S., Yamaguchi, K., and Teramoto, S., "Flowstructure of Underexpanded Jet Injected from Square Nozzle," ISABE Paper 2003-1118, 2003.

[5] Shima, E. and Jounouchi, T., "Role of CFD in Aeronautical Engineering (No. 14) - AUSM type Upwind Schemes -," *Proceedings of the 14th NAL Symposium on Aircraft Computational Aerodynamics*, NAL, Tokyo, Japan, 1997, pp. 7–12.

[6] Obayashi, S., Matsushima, K., Fujii, K., and Kuwahara, K., "Improvements in Efficiency and Reliability for Navier-Stokes Computations Using the LU-ADI Factorization Algorithm," AIAA Paper 86-0338, 1986.

[7] Fujii, K., "Unified Zonal Method Based on the Fortified Solution Algorithm," *Journal of Computational Physics*, Vol. 118, 1995, pp. 92–108.

[8] Lovely, D. and Haimes, R., "Shock Detection from Computational Fluid Dynamics Results," AIAA Paper 99-3285, 1999.

[9] Cebral, J. and Löhner, R., "Visualization on Unstructured Grids using Geometrical Cuts, Vortex Detection and Shock Surfaces," AIAA Paper 2001-0915, 2001.

[10] Pagendarm, H. and Seitz, B., "An Algorithm for Detection and Visualization of Discontinuities in Scientific Data Fields Applied to Flow Data with Shock Waves," *Scientific Visualization - Advanced Software Techniques* -, Ellis Hortwood, New York, 1993, pp. 161–177.

[11] Yanagawa, K., Fujita, T., Miyajima, H., and Kishimoto, K., "High Altitude Simulation Tests of LOX-LH2 Engine LE-5," *Journal of Propulsion and Power*, Vol. 1, No. 3, 1980, pp. 180–186.